Ballistic performance of angle-interlock woven fabrics

Ballistic performance of angle-interlock woven fabrics

Dan Yang[a]*, Xiaogang Chen[b], Danmei Sun[c], Shangyong Zhang[a], Changhai Yi[a], Xiaozhou Gong[a], Yi Zhou[a] and Yang Chen[d]

[a]Department of Textile Science and Engineering, College of Textile and Material Engineering, Wuhan Textile University, Wuhan, P. R. China;
[b]Department of Textile Engineering and Materials, School of Materials, University of Manchester, Manchester, UK;
[c]School of Textiles & Design, Heriot-Watt University, Edinburgh, UK;
[d]Department of Electronic Engineering, School of Information Science and Engineering, Changzhou University, Changzhou, P.R. China

The purpose of this paper is to investigate the ballistic performance of angle-interlock woven fabrics. Different fabric structures firstly have been compared to benchmark the ballistic performance of angle-interlock woven fabrics using the energy loss test. It has been shown that compared with other woven structures, angle-interlock woven fabric demonstrates low ballistic resistance as absorbing less impact energy. This is because angle-interlock woven fabric owns less interlacements than its counterparts. The interlacement plays an important role to help to transfer energy to the adjacent yarns: the more interlacements, the larger area the stress wave could propagate, and more projectile impact energy could be absorbed. After this systemic analysis of overall ballistic performance, more detailed parametric study of angle-interlock woven fabric is carried out. A group of 16 different structures have been tested and compared using the in-house firing range. The studies have revealed that the 3D angle-interlock woven fabric not only displays normal features of energy absorption mechanism, like yarn slippage, fibre fracture and cone formation, which 2D fabric usually demonstrates, but also shows the new property: the weaker gripping power on the constituent yarns. Besides, it also shows that the structural parameters of angle-interlock fabrics do not have a clear influence on the ballistic performance, due to the complicated factors which also have been theoretically explained from the four aspects: (a) the clamping state; (b) yarns hit by the projectile; (c) the impact angle of the projectile; (d) the impact velocity.

Keywords: angle-interlock; energy absorption; interlacement; ballistic performance; parametric study

Background

The angle-interlock woven fabric is a kind of unique 3D fabric of good mouldability. It has the advantages to shape the high mouldable ballistic application, such as the helmet (Mih, Roedel, Zahid, & Chen, 2012; Roedel & Chen, 2007; Zahid & Chen, 2013a, 2013b, 2013c, 2013d, 2014). However, the ballistic performance is very important to investigate if the candidate is selected against the ballistic impact at the same time. The ballistic performance of the angle-interlock woven fabrics therefore is firstly investigated in comparison with that of other different woven structure fabrics and further analysed in detail under the parametric studies using the energy loss test.

Impact classification

The manner in which the fabric responds to impact loading and dissipates the kinetic energy of an impacting projectile is a complex issue, which varies under different impact conditions. In simple terms, an impact with the same impact energy may happen with two separate situations: low-velocity impact by a large mass (drop weight) and high-velocity impact by a small mass (debris, bullet, etc.). The former is generally simulated using a falling weight or a swinging pendulum and the latter using a gas gun or some other ballistic launcher (Cantwell & Morton, 1991; Jayasundara, 2012). In this research, the ballistic performance of angle-interlock woven fabric will be assessed under the high-velocity impact.

Energy absorption mechanism

When the projectile hits the fabric, two waves take place (Cork & Foster, 2007; Wang, Chen, Young, & Kinloch, 2016). One is the longitudinal wave travelling in the plane of the target plate. This wave travels through the yarns which are directly hit by the projectile, known as primary yarns. The yarns not directly hit by the projectile are known as secondary yarns, which are also travelled through by this wave because they interact with the primary yarns (Kirkwood et al., 2004). Another wave, known as the transverse wave, propagates outwards from the impact zone to make deformation in the perpendicular direction to the fabric plane. The fabric deformation due to the transverse wave is shaped like a cone with the impact point at its vertex (Chocron et al., 2010; Cork & Foster, 2007). Figure 1 depicts the propagation of the two waves (Naik, Shrirao, & Reddy, 2006).

Impact energy could be converted into various forms, including yarn failure, fibre pull-out, fibre fracture, cone formation on the back face of the target and so on (Cantwell & Morton, 1991; Kirkwood et al., 2004; Naik et al., 2006). The impact energy conversion is governed by several factors, such as the material properties of the constituent fibres, boundary conditions of the sample fabric, projectile geometry and so on. Among all these, friction between yarns is quite important. The increase in friction between yarns may require more impact energy to overcome and therefore will lead to the increase in the ability to absorb the impact energy (Backman & Goldsmith, 1978). However, it must also be noticed that if the friction is so high that the relative movement of yarns is impossible, the fabrics' capability of absorbing impact energy could be correspondingly reduced. This is because the yarn movement is also an important way of absorbing the impact energy (Reedy, 1983).

Loss of kinetic energy

In principle, the energy absorbed by the target fabric on penetration assessing the ballistic performance of fabric is measured by the decrease in projectile kinetic energy, which is determined from the projectile impact velocity and the exit velocity. The overall loss of kinetic energy of the projectile is defined as (Cork & Foster, 2007):

$$\Delta E = \frac{1}{2}(mV_0^2) - \frac{1}{2}(mV_1^2) \qquad (1)$$

where ΔE is the loss of kinetic energy; m is the projectile mass; V_0 is the impact velocity; V_1 is the exit velocity.

The impact velocity V_0 can be calculated from the flying time of the projectile t_0 between two detectors placed at d_0 distance apart. The impact velocity V_0 can be then calculated from

$$V_0 = \frac{d_0}{t_0} \qquad (2)$$

The exit velocity V_1 can be achieved using the same method, by measuring projectile flying time t_1 between the two detectors with a distance d_1 between them behind the target fabric. After that, the overall loss of kinetic energy carried by the projectile can be calculated according to Equation (1). The energy loss of the projectile is an effective way to measure fabric's capability of absorbing energy which is difficult to measure directly.

(a)　　　　　　　　　　　　(b)
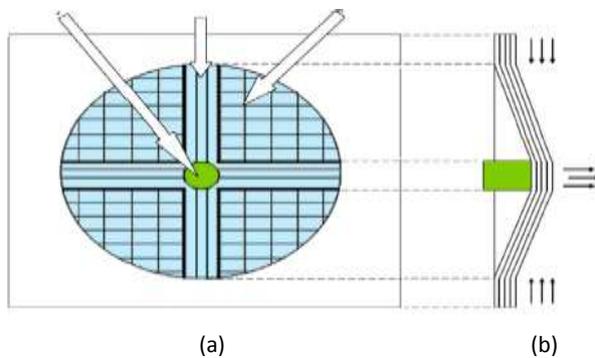
Figure 1 Impact wave propagation: (a) top view; (b) side view.

In comparison to other fabric structures in energy absorption

Fabrics for test

Structures

Plain weave. Plain weave is the simplest weave, characterized by the tightest woven structure. It is a largely, widely used woven structure in the application. Plain weave with leno insertions. Leno weave is a type of structure that a pair of warp yarns is intertwined by embracing a pick of weft yarn in each of the interstices (Grosicki, 1977). It has firmer gripping on the weft yarns and can be produced easily in broad fabrics. The primary purpose of such structure is to limit yarn movement, and therefore, the fabrics with stable dimensions can be formed. The plain weave fabrics with leno insertions are expected to have better dimensional stability than that without leno insertions, and should have better restraining on the weft yarns. Figure 2 shows the leno weave structure.

Figure 2. Illustration of leno weave.

Figure 3. Weft yarn cramming.
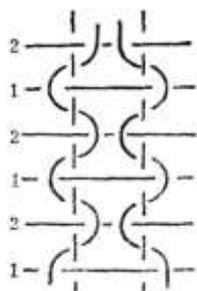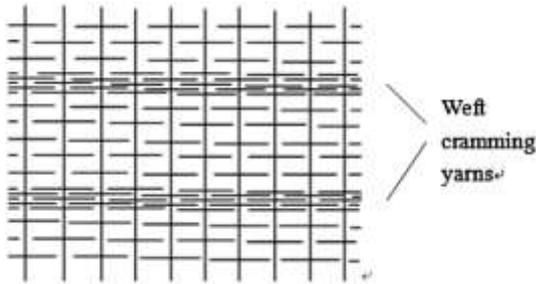
Plain weave with weft yarn cramming. Weft yarn cramming in weaving is performed by stopping take-up, at the same time keeping all other actions as usual during weaving. Fabric weave structure keeps the same. Weft yarn density increases when weft yarn cramming takes place, as shown in Figure 3.

Four-layer cellular fabric. The four-layer cellular fabric with plain weave structure is shown in Figure 4. This is performed by connecting the adjacent two layers together in the evenly spaced intervals. Eight warp yarns and 104 weft yarns compose one repeat unit of the weave structure. The conjunction area is characterized by eight weft yarns and twice the yarn density in both warp and weft directions.

Figure 4. Four-layered cellular fabric.

Specimen details

Twenty-one different woven fabrics have been designed and manufactured. The detailed specifications are listed in Table 1. The fabrics were then cut into the size of 24 cm by 24 cm, clamped by a pair of metal clamps for energy loss test. As shown in Figure 5, needles, which were planted onto one part of the clamp around an aperture with the diameter of 15.2 cm, were used to lock the target area by penetrating the fabric. The target area was further guaranteed by screwing the two clamps together in the four corners. This full-clamped state was suggested to offer the same condition for all the tests.

Experiments
The energy loss test was used to investigate the fabrics' ballistic performance. The firing range for energy loss test consists of a firing device with a 7.6 mm rifle barrel, the target holder and velocity detectors. These are arranged in an enclosed environment and the firing apparatus is shown in Figure 6.

Table 1. Specifications of various fabrics.

Fabrics	Note	Fibre type	Yarn densities		Yarn counts	
			Warp (ends/cm)	Weft (picks/cm)	Warp (tex)	Weft (tex)
BPLAIN	Broad plain woven fabric					
BPL02	Broad plain woven fabric with leno insertions in every 2-cm intervals					
BPL02WC	Broad plain woven fabric with leno insertions in warp and cramming yarns in weft both in every 2-cm intervals					
BPL04	Broad plain woven fabric with leno insertions in every 4-cm intervals					
BPL04WC	Broad plain woven fabric with leno insertions in warp and cramming yarns in weft both in every 4-cm intervals					
BPL06	Broad plain woven fabric with leno insertions in every 6-cm intervals					

Code	Description	Material				
BPL06WC	Broad plain woven fabric with leno insertions in warp and cramming yarns in weft both in every 6-cm intervals					
BPL08	Leno structure is designed in every 8 cm (64ends) intervals along fabric width.					
BPL08WC	Broad plain woven fabric with leno insertions in warp and cramming yarns in weft both in every 8-cm intervals					
BPL10	Leno structure is designed in every 10 cm (80ends) intervals along fabric width	Kevlar49®	7.5	7.5	158	158
BPL10WC	Leno and cramming weft are in every 10 cm (80ends/picks) intervals, respectively.					
B2LRE	Two layers joint in one with 8 weft yarns in every 48 weft yarns intervals along fabric length					
B2LIN	Two layers joint in one with 8 weft yarns in every 48 weft yarns intervals along fabric length, the two layers exchange in each joint					
B4LRE	Broad plain woven regular four-layer fabric					
HPWW06	Handloom-made plain woven fabric with weft winding in every 6-cm intervals					
4LAI12 × 26	Four layer angle-interlock fabric with densities 12 ends/cm and 26 picks/cm			26		
4LAI12 × 28	Four layer angle-interlock fabric with densities 12 ends/cm and 28 picks/cm		12	28		
4LAI12 × 30	Four layer angle-interlock fabric with densities 12 ends/cm and 30 picks/cm			30		
BDP	Broad plain woven fabric					
BDPL04	Leno is in every 4cm intervals along fabric width	Dyneema®	6.73	6.73	176	176
BDUD	Broad unidirectional fabric					
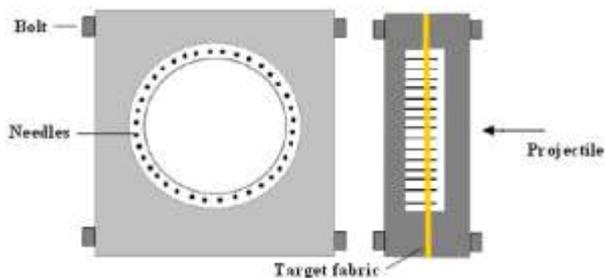
Figure 5. Fabric clamp.

Figure 6. Testing apparatus.

A blank cartridge was used to propel the projectile held in a sabot. The projectile is a steel cylinder with a diameter and a length of being both 5.56 mm, weighing 1.06 g, as shown in Figure 7(a). Pulling the trigger causes the projectile to be forced out from the barrel towards the target fabric at a high velocity, typically 480 m/s. The time detectors then picked up the travelling time of the projectile before and after the fabric target. The loss in kinetic energy carried by the projectile after

4

going through the fabric can be calculated using Equation (1). In this set-up, the distances between the two pairs of time detectors were 47 cm (front) and 36.2 cm (rear), respectively. Figure 7(c) sketches the construction of this firing range.

Figure 7. Construction of the testing apparatus: (a) steel projectile; (b) plastic sabot; (c) schematic diagram.
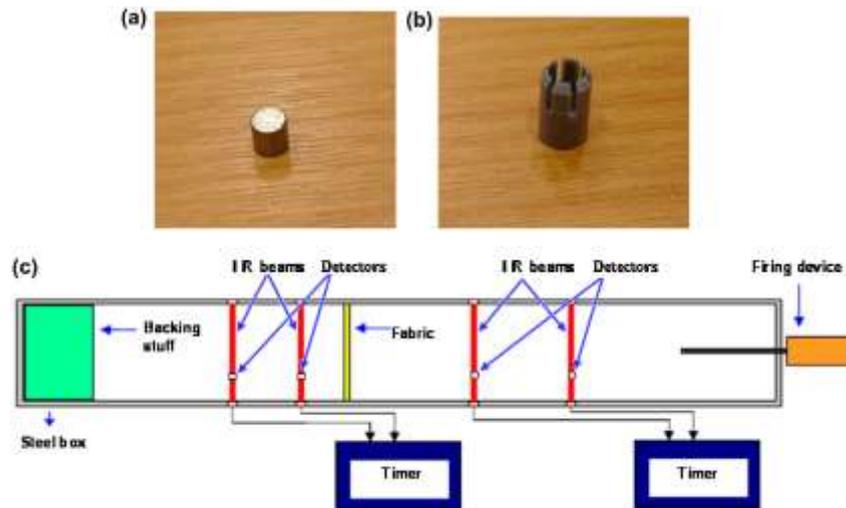
Test results and analysis

Figure 8 shows the results of energy loss test for all fabrics. To indicate the energy loss caused by the same amount of materials, the projectile energy loss in Figure 8 is normalized by dividing the fabric areal density (in g/cm^2). Relatively speaking, the overall ballistic performance of angle-interlock woven fabrics is quite low as 4LAI12 × 26, 4LAI12 × 30, 4LAI12 × 32 and 4LAI12 × 28 are ranked as the 1st, 2nd, 3rd and 5th, respectively, from the bottom. All the 2D woven fabrics have shown capabilities to absorb more energy than the 3D angle-interlock woven fabrics. This is believed to be due to the difference of the number of interlacements contained in the fabrics, which is directly related to the yarn gripping effect. More interlacements lead to tighter yarn gripping. There are more yarn interlacements in 2D woven fabric per unit area compared to 3D angle-interlock woven fabric per unit area; and the interlacements help to transfer energy to the adjacent yarns. Consequently, the stress wave in 2D plain woven fabric propagates to a larger area of woven fabric, whereas that in 3D angle-interlock woven fabric tends to be more localized. As a result, the 2D plain woven fabric would absorb more projectile impact energy than the 3D angle-interlock woven fabric.

As the plain woven fabric is the conventional type, it is of interest to compare the angle-interlock woven fabrics with the plain woven fabrics to benchmark the ballistic performance of the angle-interlock woven fabrics. As can be seen in Figure 8, the plain woven fabrics absorb more kinetic energy than the angle-interlock woven fabrics. The top view of structures of plain and four-layer angle-interlock weaves is shown in Figure 9(a) and (b), respectively. It could be observed that in the same unit area, there are more interlacements in the plain weave than the four-layer angle-interlock weave. Additionally, the former also has shown more interlacements than the latter in the cross section. Furthermore, the energy loss is normalized by dividing the fabric areal density for the purpose of comparison based on the same amount of material. Interlacements are quite important for the fabric to absorb the impact energy. Interlacements serve like pivot points to stabilize the structure in order to enhance the yarn gripping by increasing friction between yarns. When the fabric receives an impact, the impact energy will dissipate among the warp and weft yarns, and will be distributed on interlacements for further dissipation. More interlacements may make the energy distribution and dissipation more effectively because better gripping of yarns in the fabric helps the impact energy to propagate to a larger area of fabric. Nevertheless, the energy absorption mechanism is a complicated procedure influenced not only by friction but also by other factors. It is necessary to mention that if the friction between yarns is too high, e.g. to a level that blocks the yarn movement in the fabric, the impact energy absorption by yarns displacement will be minimized, and the mechanism for the energy to be absorbed is left to the yarn breakage only. This is the reason that the unidirectional fabric (BDUD) made from high performance polyethylene demonstrated lower energy absorption on weight basis than the single-layer woven fabrics (e.g. BDPL04, 1 × BPlain, BDP, etc.) and even than a certain type of angle-interlock woven fabrics (4LAI12 × 28), as shown in Figure 8.
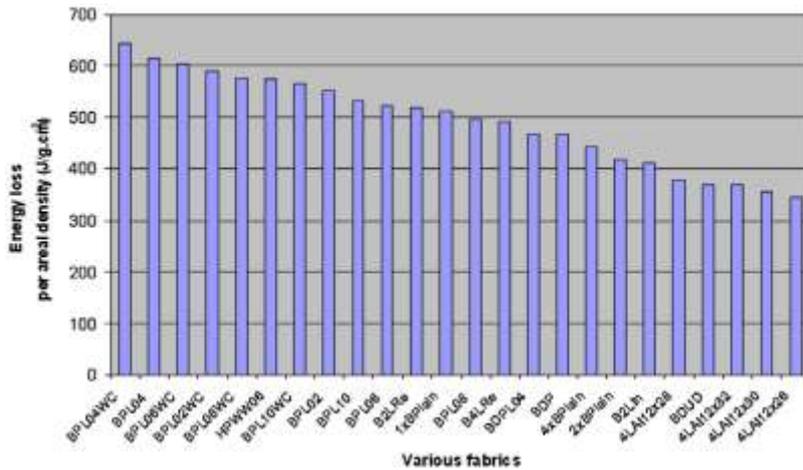
5

Figure 8. Energy absorption of various fabrics normalized by per areal density.
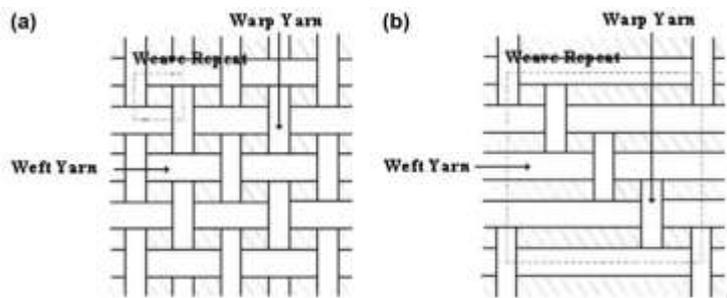

Figure 9. Weave structure: (a) plain; (b) four-layer angle-interlock.

Additionally, based on all the designed and manufactured fabrics so far, comparisons are also made on other various fabrics' ability in absorbing impact energy. Important findings are listed as follows:

- Fabrics with leno insertions in warp and cramming yarns in weft show better performance of impact energy absorption than their counterparts without weft yarn cramming. BPL04WC (Broad plain woven fabric with leno insertions in warp and cramming yarns in weft both in every 4-cm intervals) is the best in terms of impact energy absorption. This is because weft yarn cramming could also improve the yarn gripping effect to increase friction among weft yarns by increasing weft density. More kinetic energy is consumed against this additional friction. However, for BPLWC fabric itself, optimal setting exits; in this research, fabrics with 4-cm insertion intervals are better than other settings. Further investigations may be required in this specific region.
- HPWW06 (Handloom-made plain woven fabric with weft winding in every 6-cm intervals) performs better than BDPL06 (the fabric with same insertion intervals of leno weave). This may because much tighter warp yarns grip the winding weft yarns compared to leno weave structure.
- 3D cellular fabrics and the same layer 2D plain fabric: The Two- and four-layered cellular fabrics perform better than the assembly with the same layer 2D plain woven fabric of similar yarn densities.
- Dyneema® plain woven fabrics absorb less impact energy compared to their Kevlar® counterparts. These results may verify that the low surface friction of Dyneema® fibre affects its ballistic-resistant performance.
- For the unidirectional and woven Dyneema® fabrics, the former one shows reduced ballistic performance than the latter one, but may have the better trauma proof ability.

Parametric study of ballistic performance of angle-interlock woven fabrics

The above-mentioned section mainly focused on the overall ballistic performance of different woven fabrics and it showed that angle-interlock woven fabric demonstrates relatively low capabilities against the ballistic impact. For the purpose of better understanding of the ballistic resistance of angle-interlock woven fabrics, a parametric study of the angle-interlock fabrics on the ballistic performance has been further carried out.

Fabrics for test

A series of angle-interlock woven fabrics with different structural parameters, as shown in Table 2, have been produced using the Saurer 100W dobby loom with the maximum heald frames 22 and the maximum width 1.2 m under the loom speed 160 picks/minute. A negative let-off mechanism was used in controlling the weaver's beam and balancing the warp yarn tension. Kevlar® 49 with 158 tex, the commonly used yarns for ballistic protective applications, was used to make the angle-interlock woven fabrics.

6

Experiments

These fabrics were ballistically tested in the clamped state for energy absorption at the room temperature using the firing apparatus. Before coming to the test result analysis, it is necessary to mention that features displayed in 2D woven fabrics such as the yarn slippage, the fibre fracture and the cone formation can also be identified in 3D angle-interlock woven fabrics during the ballistic test.

Observations

Figure 10(a) shows a typical sample after shooting when the clamp has been removed. It can be seen that some of the primary yarns are broken, whilst some others are pulled towards the impact point where the projectile has penetrated the target fabric. The arrows signify the direction of primary yarn motion. This is similar to the situation where a single-layer plain woven fabric is impacted on, where the longitudinal and transverse waves would be generated. Primary yarns stand the ballistic impact directly, which, however, could not consume a lot of kinetic energy and therefore exhibits fracture and pull-out as two typical localized damages in the central impact zone, as shown in Figure 10(a). Another apparent phenomenon is the pulling of the primary yarns from the fabric edge, more serious than the situation for the plain woven fabrics. This indicates that the angle-interlock woven fabrics have lower gripping power to the constituent yarns because of the fabric structure. Thirdly, cone formation phenomenon is quite noticeable. As a matter of fact, the conic shape seen in Figure 10(a) is not the cone caused by the transverse movement of the projectile. It is rather a combination of the actions from the impact of the projectile, the sabot and the oscillation of the fabric. The cone formation caused by the projectile takes place in a very short period after the impact (a few microseconds). The fabric works like a net to block the flying projectile, which performs a conical deformation towards backface of the target fabric; at the top of the cone, localized damage takes place. Like other types of ballistic fabrics, fabric areas associated to the secondary yarns are not much affected by the impact. Measures need to be taken to get more of such areas to be involved in absorbing energy. Efforts are being made to improve the situation of ballistic fabrics, described in Section 'In comparison to other fabric structures in energy absorption'. The property of low shear rigidity of angle-interlock woven fabric is determined by its unique structure consisting of layers of straight weft yarns bound by a single layer of warp yarns from back to face. Generally speaking, the angle-interlock woven fabric displays not only normal features of energy absorption mechanism but also new characteristics, e.g. low gripping on yarns. However, as angle-interlock woven fabrics have a multi-layer of straight weft yarns, they should be able to take on the impact more directly by yarns than other types of fabrics if the gripping on yarns can be improved. This remains to be explored for future research along this line.

Table 2. Fabric specifications.

| Fabrics	Fibre type	Yarn density		Yarn count		Areal density
		Warp (ends/cm)	Weft (picks/cm)	Warp (tex)	Weft (tex)	(g/m²)
4LAI12 × 26			26			609.02
4LAI12 × 28		12	28			28 640.58
4LAI12 × 30			30			672.13
4LAI12 × 32			32			703.69
5LAI8 × 26	Kevlar® 49		26			542.76
5LAI8 × 28		8	28			574.31
5LAI8 × 30			30			605.87
5LAI8 × 32			32			637.42
5LAI10 × 28			28	158	158	607.44
5LAI10 × 30		10	30			639.00
5LAI10 × 32			32			702.11
5LAI12 × 26			26			609.02
5LAI12 × 28		12	28			640.58
5LAI12 × 30			30			672.13
5LAI12 × 32			32			703.69
5LAI12 × 34			34			735.24
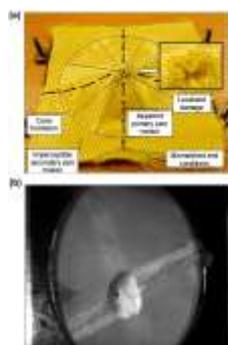
Figure 10. The impacted fabric (a) the final state (b) during the impact (snapshot).

Test results and analysis

Data processing

The original data obtained during the energy loss test are attached as Appendix 1. The t_0, the time used by the projectile to travel through a pair of detectors before impact, and t1, the time used to travel through the detectors after impact, were the original data caught during the energy loss test. Due to the importance of the data, the following actions were taken to eliminate the less meaningful from the data-set.

(1) For each sample group, the t_0 and t_1 were averaged, respectively. Data were only selected if they were within ±10% of the average values.

(2) The selected values for t0 and t1 were averaged again, respectively. The average data were employed to calculate the impact and exit velocities and the energy loss using Equations (2) and (1), respectively, mentioned in Section 'Loss of kinetic energy'.

The results after data selection are shown in Table 3, where V_0, V_1, E_0, E_1 and ΔE represent the impact velocity, exit velocity, impact energy carried by the projectile, residual energy carried by the projectile and the energy loss due to penetration, respectively. In order to eliminate the effect of the amount of fibre materials in each of the fabrics, the energy loss was normalized by the areal density for the purpose of comparisons.

This study aimed to examine the influence of structure on the energy loss. Structural parameters considered include the number weft yarn layer, weft density and warp density of the angle-interlock fabrics.
The relationships are depicted in Figure 11.

Table 3. Ballistic results.

Fabrics	Areal density (g/m²)	V_0 (m/s)	V_1 (m/s)	E_0 (J)	E_1 (J)	ΔE (J)	$\dfrac{\Delta E}{\text{Areal density}}$(J.g/cm²)
4LAI12 × 26	609.02	483.04	439.99	123.63	102.57	21.06	345.80
4LAI12 × 28	640.58	469.65	418.14	116.87	92.64	24.23	378.25
4LAI12 × 30	672.13	486.04	437.20	125.17	101.28	23.89	355.44
4LAI12 × 32	703.69	483.66	429.93	123.95	97.94	26.01	369.62
5LAI8 × 26	542.76	466.58	422.24	115.35	94.47	20.88	384.70
5LAI8 × 28	574.31	477.84	440.28	120.98	102.71	18.27	318.12
5LAI8 × 30	605.87	494.51	451.05	129.57	107.80	21.78	359.48
5LAI8 × 32	637.42	485.91	444.72	125.10	104.79	20.31	318.63
5LAI10 × 28	607.44	501.07	447.10	133.03	105.92	27.11	446.30
5LAI10 × 30	639.00	480.57	420.83	122.37	93.84	28.53	446.48
5LAI10 × 32	702.11	476.75	417.93	120.43	92.55	27.88	397.09
5LAI12 × 26	609.02	485.24	428.71	124.76	97.38	27.37	449.41
5LAI12 × 28	640.58	513.47	473.62	139.70	118.85	20.85	325.49
5LAI12 × 30	672.13	478.25	434.70	121.19	100.12	21.06	313.33
5LAI12 × 32	703.69	492.04	429.01	128.28	97.52	30.76	437.12
5LAI12 × 34	735.24	489.07	444.06	126.74	104.48	22.25	302.62

Analysis

It could be seen from Figure 11 that the trend in all cases is not clearly obvious. This section will try to give explanations from four different angles, which are (a) the clamping state; (b) yarns hit by the projectile; (c) the impact angle of the projectile; (d) the impact velocity.
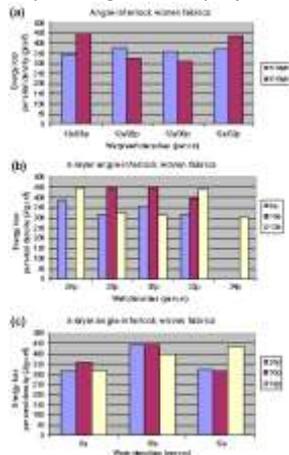

Figure 11. Energy loss normalized by areal density vs. parameters: (a) weft layers; (b) weft densities; (c) warp densities.
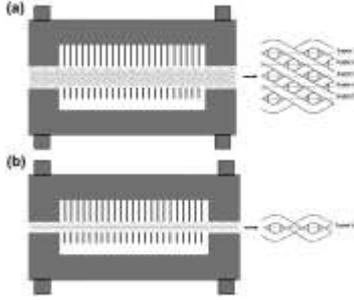
8

Figure 12. Clamping state: (a) five-layer angle-interlock woven fabric; (b) plain woven fabric.

Clamping. Fabric clamping is important as boundary conditions influence the ballistic performance of the fabrics. Fabrics were clamped for energy loss test, and the clamp held the fabric by four fastening screws in the corners of the clamp with needles evenly distributed in a circular arrangement, as shown in Figure 5. However, an angle-interlock woven fabric contains multiple layers of weft yarns leading to a thick fabric, and that requires more clamping power, compared to the situation of clamping the single-layer 2D woven fabric. Figure 12 illustrates the clamping of the five-layer angle-interlock woven fabric and the single-layer plain woven fabric for comparison. The thickness of the former is almost five times than the latter, which indicates that the angle-interlock woven fabric requires much more clamping power to be stabilized, and therefore, it is more difficult to be clamped well. Additionally, the weft yarns in the angle-interlock fabric are straight and only interlaced with a single layer of warp yarns. Therefore, the weft yarns are not well gripped by the fabric and hence easy to move. This makes tight clamping more difficult. The difficulty to offer the exact unified clamping state may be an important factor leading to the randomness of results.

Yarns hit by the projectile. The number of warp/weft yarns hit by the projectile may lead to the complication of energy absorption of the fabric. In a fabric, the spot the projectile hits is composed by warp and weft yarns. The projectile may hit the yarns, the interlacements or the gap between yarns. If the projectile hits quite a few yarns, the results will be quite complicated. In an ideal situation where the whole end area of the projectile touches the fabric, the numbers of warp and weft yarns hit by the projectile, denoted as N_e and N_p, respectively, can be calculated as follows:

$$N_e = \frac{d_{pro}}{d_e} \qquad (3)$$

$$N_e = \frac{d_{pro}}{d_{pl}} \times n_l \qquad (4)$$

where d_{pro} is the diameter of the projectile; d_e is the distance between the neighbouring warp yarns; d_{pl} is the distance between the neighbouring weft yarns per weft layer as the angle-interlock woven fabric has a multilayer structure; and n_l is the number of weft layers.

Figure 13 illustrates the impact area hit by the projectile on the angle-interlock woven fabric. The impacted fabric area is equal to the end area of the projectile. Therefore, the diameter of the projectile d_{pro} would determine the length and width of the fabric which is impacted on. D_{pro}/d_e and d_{pro}/d_{pl} give the numbers of warp and weft yarns directly hit by the projectile. The latter value needs to multiply the number of weft layers, nl, to obtain the total number of weft yarns influenced by the projectile as the thickness of the angle-interlock woven fabric is
considered.

d_e and d_{pl} could be achieved by:

$$d_e = \frac{1}{n_e} \qquad (5)$$

$$d_{pl} = \frac{n_l}{n_p} \qquad (6)$$

where n_e and n_p are the warp/weft density. Substituting (5) and (6) into (3) and (4), respectively, leads to

$$N_e = d_{pro} . n_e \qquad (7)$$

9

$$N_p = \frac{d_{pro} \cdot n_p}{n_1} \qquad (8)$$

Taking four-layer angle-interlock woven fabric with 12 ends/cm and 26 picks/cm as an example (the relative details are shown in Table 2), the number of warp and weft yarns covered by the end area of the projectile, N_e and N_p, can be easily calculated as 7 and 15, respectively.
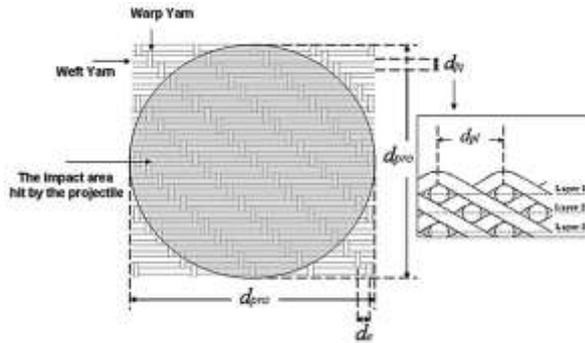

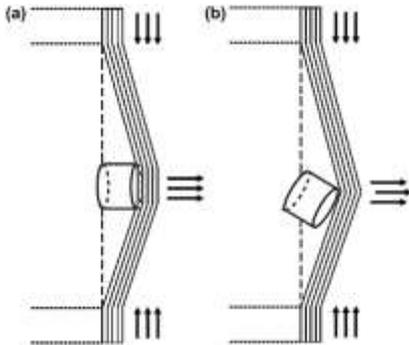Figure 13. The impact area hit by the projectile.

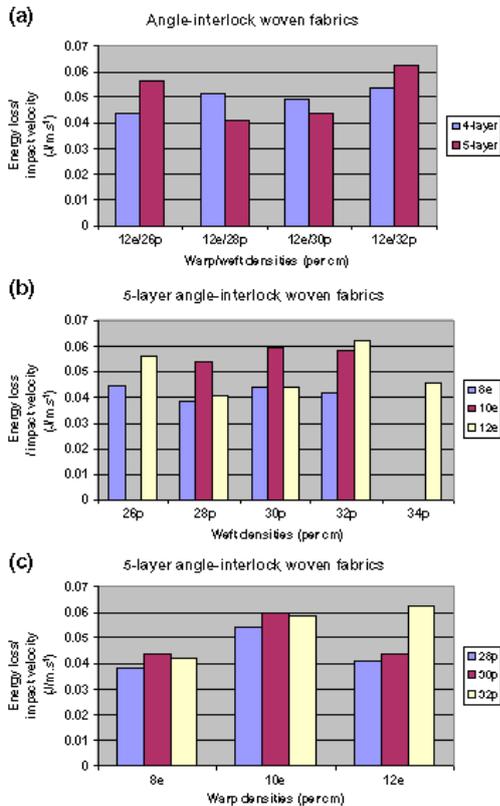Figure 14. Portions of projectile when impacting the fabric: (a) full-end section; (b) edge segment.

Figure 15. Energy loss normalized by impact velocity vs. parameters: (a) weft layers; (b) weft densities; (c) warp densities.

10

This indicates that for this fabric, the projectile needs to work directly with 7 ends and 15 picks during the ballistic impact. More possibilities will be created when more yarns are under the attack. Failure of a yarn at a different location will cause a different reaction from the rest of the yarns. It can be said in general that the consideration of the numbers of warp and weft yarns hit by the projectile contributes to the uncertainty in the ballistic results.

The impact angle of the projectile. The above-mentioned analysis is considered under the ideal state where the flat end of the cylindrical projectile perfectly hits the target fabric for all the experiments, as shown in Figure 14(a). However, in the real situations, the projectile may impact on the fabrics in any orientation as indicated in Figure 14(b); consequently, the randomness of the kinetic energy absorption by the fabric will occur. It is well accepted that the smaller the impact area, the larger the stress will be caused in the fabric when the identical force is applied to the fabric based on the definition of stress. Stress is a measure of the average amount of force exerted per unit area of a surface within a deformable object (The Wikipedia, 2016):

$$\sigma = \frac{F}{A} \qquad (8)$$

where σ is the stress; F is the total tensile or compressive force; A is the area where force acts upon.
According to this principle, the force-exerted area is larger in Figure 14(a) than in Figure 14(b) since in the former case the end of the cylinder fully touches the fabric, which results in smaller stress and hence smaller strain in the fabric. More energy will have to be used to cause a bigger strain in the fabric in order to break the fabric. Consequently, the exit velocity will be lower and the energy loss will be larger based on Equation (1), when all other conditions are supposed to be unchanged. The different angles of projectile hitting the fabric would lead to the difference in energy loss.

The impact velocity. The impact velocity may also have affected the results of the ballistic impact. During the impact test, it was seen that the impact velocity V_0 fluctuated from round to round of shootings, as demonstrated in Table 3. This is mainly due to the variation in the amount of explosive powder in the cartridges. It seems not likely to have exactly the same explosion every time. Therefore, keeping the impact velocity V0 constant seems hard to achieve. As an attempt to eliminate the influence of the variation in velocity, the energy loss results normalized by the impact velocity V_0 are shown in Figure 15. Comparison between Figures 11(c) and 15(c) does show that the projectile velocity influences the energy loss. The reasons for the randomness of the energy loss results are quite complicated. Apart from the abovementioned possibilities, the intrinsic factors could not be neglected, such as the yarn count, materials of the yarns and weave structure which is considered to be fundamental. The structure of angle-interlock woven fabrics is composed of several layers of straight inserted weft yarns interlaced with a single layer of warp yarns from face to back. Low shear rigidity is its apparent character which indicates yarns are easy to move within the fabric under the impact. Besides, the angle-interlock woven fabric has a multi-layer structure; the thickness of the fabric could add more possibilities in ways energy is absorbed by the fabric. Further investigations may be required to address this issue.

Conclusions

This paper has focused on the ballistic performance of angle-interlock woven fabrics and it shows that this kind of fabric demonstrates relatively low capabilities absorbing the impact energy, compared with fabrics of other structures. This is mainly determined by angle-interlock woven fabric structure; which consists of layers of weft yarns laid straight and bound by a single layer of warp yarns to lock the layers of weft yarns together. This unique structure leads to less interlacements which, however, limits the stress wave propagation in the fabric when against the high-velocity impact. For the continuous research, this paper has further investigated angle-interlock woven fabric itself via parametric study of ballistic performance. It has reported the outcome from the energy loss test of the angle-interlock fabrics with the aim to find the strongest candidate against the high velocity ballistic impact. However, after the group of 16 parameters systematically designed, tested, compared and analysed, a clear tendency is difficult to be found. This is mainly due to the unique multi-layer combined structure of angle-interlock woven structure which leads to the difficulty of tight clamping, and the random yarns hit by the projectile. Meanwhile, this complication is increased by the difference of the impact angle of projectile, and the influence of the variation in velocity. The more systematic parameters and the improved test method may be required to investigate in the future research.

Disclosure statement
No potential conflict of interest was reported by the authors.

References

Backman, M. E., & Goldsmith, W. (1978). The mechanics of penetration of projectiles into targets. International Journal of Engineering Science, 16, 1–99.
Cantwell, W. J., & Morton, J. (1991). The impact resistance of composite materials – A review. Composites, 22, 347–362.
Chocron, S., Figueroa, E., King, N., Kirchdoerfer, T., Nicholls, A. E., Sagebiel, E., … Freitas, C. J. (2010). Modeling and validation of full fabric targets under ballistic impact. Composites Science and Technology, 70, 2012–2022.

Cork, C. R., & Foster, P. W. (2007). The ballistic performance of narrow fabrics. International Journal of Impact Engineering, 34, 495–508.

Grosicki, Z. (1977). Watson's advanced textile design: Compound woven structures. London: Butterworth & Ltd.

Jayasundara, H. (2012). Impact resistance of composite materials (MSC thesis). Manchester: University of Manchester.

Kirkwood, J. E., Kirkwood, K. M., Lee, Y. S., Egres, R. G., Wagner, N. J., & Wetzel, E. D. (2004). Yarn pull-out as a mechanism for dissipating ballistic impact energy in Kevlar (R) KM-2 Fabric: Part II: Predicting ballistic performance. Textile Research Journal, 74, 939–948.

Mih, S., Roedel, C., Zahid, B., & Chen, X. (2012). Moulding of single-piece woven fabrics for protective helmets – A review and future work. 4th World Conference on 3D Fabrics and Their Applications, TexEng/RWTH Aachen, Aachen.

Naik, N. K., Shrirao, P., & Reddy, B. C. K. (2006). Ballistic impact behaviour of woven fabric composites: Formulation. International Journal of Impact Engineering, 32, 1521–1552.

Reedy, J. N. (1983). Impact on laminated composite plates: A review of recent computational developments. Proceedings of the Army Research Office Workshop on Computational Aspects of Penetration Mechanics, Aberdeen.

Roedel, C., & Chen, X. (2007). Innovation and analysis of police riot helmets with continuous textile reinforcement for improved protection. Journal of Information and Computing Science, 2, 127–136.

The Wikipedia. (2016). Retrieved from https://en.wikipedia.org/ wiki/Tensile_testing#CITEREFDavis2004

Wang, Y., Chen, X., Young, R., & Kinloch, I. (2016). A numerical and experimental analysis of the influence of crimp on ballistic impact response of woven fabrics. Composite Structures, 140, 44–52.

Zahid, B., & Chen, X. (2013). Energy absorption at different impact locations of riot helmet shells. International Journal of Textile Science, 2, 126–131.

Zahid, B., & Chen, X. (2013). Properties of 5-layer angle-interlock Kevlar-based composite structure manufactured from vacuum bagging. Journal of Composite Materials, 47, 3227–3234.

Zahid, B., & Chen, X. (2013). Manufacturing of single-piece textile reinforced riot helmet shell from vacuum bagging. Journal of Composite Materials, 47, 2342–2351.

Zahid, B., & Chen, X. (2013). Development of a helmet test rig for continuously textile reinforced riot helmets. International Journal of Textile Science, 2, 12–20.

Zahid, B., & Chen, X. (2014). Impact performance of singlepiece continuously textile reinforced riot helmet shells. Journal of Composite Materials, 48, 761–766.

Appendix 1. Original data obtained during the energy loss test

Fabrics	Fabric 1		Fabric 2		Fabric 3		Fabric 4		Fabric 5		Fabric 6	
	t_0^*	t_1^{**}	t_0	t_1	t_0	t_1	t_0	t_1	t_0	t_1	t_0	t_1
4LAJ12×26	0.981	0.831	0.962	0.801	1.017	0.931	0.958	0.79	0.991	0.869		
4LAJ12×28	1.03	0.916	0.962	0.826	1.072	0.919	1.129	0.983	0.939	0.802	0.931	0.776
4LAJ12×30	0.957	0.828	0.942	0.778	0.905	0.776	1.009	0.977	1.054	0.986	1.054	0.986
4LAJ12×32	1.046	0.967	0.952	0.801	0.912	0.754	0.977	0.846				
5LAJ8×26	1.103	1.093	0.948	0.797	1.081	0.904	0.932	0.771	0.993	0.871		
5LAJ8×28	0.956	0.823	0.994	0.858	0.94	0.768	1.027	0.837	1.001	0.825		
5LAJ8×30	0.915	0.745	1.023	0.929	0.919	0.767	0.934	0.789	0.999	0.835		
5LAJ8×32	0.927	0.784	0.894	0.741	1.022	0.812	1.026	0.919				
5LAJ10×28	0.944	0.812	0.945	0.815	0.925	0.802						
5LAJ10×30	0.867	0.731	1.04	1.016	1.02	0.955	0.9	0.737	0.985	0.862		
5LAJ10×32	1.023	0.993	0.946	0.782	0.914	0.778	0.995	0.886	1.045	0.874	0.992	0.884
5LAJ12×26	0.956	0.824	0.968	0.838	0.907	0.76	1.101	1.053	0.936	0.799	1.076	1.001
5LAJ12×28	0.903	0.756	0.856	0.705	N/A	0	0.987	0.832				
5LAJ12×30	N/A	0	0.985	0.877	N/A	0	0.99	0.817	1.017	0.849	0.939	0.788
5LAJ12×32	0.924	0.799	0.978	0.875	N/A	0	0.974	0.875	0.968	0.855	0.932	0.815
5LAJ12×34	0.932	0.767	0.993	0.841	0.968	0.873	0.958	0.795	0.954	0.8		

t_0^*: the time used by the projectile to travel through a pair of detectors before the impact.

t_1^*: the time used by the projectile to travel through a pair of detectors after the impact.